Research Square

Preprints are preliminary reports that have not undergone peer review.
They should not be considered conclusive, used to inform clinical practice,
or referenced by the media as validated information.

Development and Validation of a Survival Machine Learning Model for Predicting Major Adverse Cardiovascular Events After Percutaneous Coronary Intervention in Patients With Coronary Artery Aneurysm or Ectasia

Yuhao Liu
First Affiliated Hospital of Dalian Medical University
Xiaopeng Dong
First Affiliated Hospital of Dalian Medical University
Zhichao Dong
First Affiliated Hospital of Dalian Medical University
Yuxin Yang
First Affiliated Hospital of Dalian Medical University
Bo Zhang
zhangbo@dmu.edu.cn

First Affiliated Hospital of Dalian Medical University

Research Article

Keywords: Coronary artery aneurysm, coronary artery ectasia, percutaneous coronary intervention, major adverse cardiovascular events, random survival forest, risk prediction

Posted Date: November 18th, 2026

DOI: https://doi.org/10.21203/rs.3.rs-11572812/v1

License: This work is licensed under a Creative Commons Attribution 4.0 International License.
Read Full License

Additional Declarations: No competing interests reported.

Development and Validation of a Survival Machine Learning Model for Predicting Major Adverse Cardiovascular Events After Percutaneous Coronary Intervention in Patients With Coronary Artery Aneurysm or Ectasia

Yuhao Liu[a,†], Xiaopeng Dong[a,†], Zhichao Dong[a], Yuxin Yang[a,*], Bo Zhang[a,*]

†Yuhao Liu and Xiaopeng Dong contributed equally to this work.

*Bo Zhang and Yuxin Yang are co-corresponding authors. Correspondence: Bo Zhang, zhangbo@dmu.edu.cn; Yuxin Yang, yangyuxinemc2@126.com.

[a] The First Affiliated Hospital of Dalian Medical University, Dalian, China

Abstract

Background: Patients with coronary artery aneurysm or ectasia (CAAE) remain at risk of major adverse cardiovascular events (MACE) after percutaneous coronary intervention (PCI). We aimed to develop and temporally validate a model for post-discharge MACE.

Methods: This single-centre retrospective cohort included 574 adults with angiographically confirmed CAAE who underwent PCI and survived to discharge. Patients were chronologically assigned to development (n = 456) and temporal validation (n = 118) cohorts. Missing data were handled using five MICE datasets. LASSO-Cox selected predictors, and six survival algorithms were compared using 10 repeats of stratified five-fold cross-validation. Internal validation used 1,000 patient-level bootstrap resamples with optimism correction; temporal validation was performed without refitting or recalibration.

Results: During follow-up, 85 development-cohort patients and 12 temporal-validation patients experienced MACE, including 45 and 11 patients, respectively, within 3 years. Seven predictors were retained. Random survival forest (RSF) was selected according to the prespecified rule, with the highest mean out-of-fold C-index (0.761, SD 0.038). In development, the optimism-corrected C-index and 3-year AUC were 0.813 (95% CI 0.782–0.838) and 0.847 (0.806–0.881); corresponding temporal validation estimates were 0.826 (0.734–0.910) and 0.843 (0.742–0.931). Compared with Cox, RSF improved 3-year AUC by 0.098 in development (P = 0.018) and 0.118 in temporal validation (P = 0.032).

Conclusions: RSF showed good discrimination and identified a high-risk group, with preliminary support from same-centre temporal validation. Calibration and clinical net benefit require confirmation in larger, multicentre cohorts before clinical use.

Keywords: Coronary artery aneurysm; coronary artery ectasia; percutaneous coronary intervention; major adverse cardiovascular events; random survival forest; risk prediction

Background

Coronary artery aneurysm or ectasia (CAAE) encompasses coronary artery aneurysm (CAA) and coronary artery ectasia (CAE). The two conditions have different morphological definitions, but both involve abnormal coronary dilatation.[1-3] Slow flow, local thrombosis, and distal embolization may accompany these lesions and complicate management, particularly in patients with obstructive coronary disease who undergo PCI.

Long-term cardiovascular risk in CAAE is substantial, although reported event rates vary with the population, follow-up period, and outcome definition. In the international CAAR registry of 1729 patients with CAA, 37.1% experienced MACE during a median follow-up of 44.8 months; the composite outcome included all-cause death, heart failure, unstable angina, and recurrent myocardial infarction.[4] Among patients with acute myocardial infarction, the 4-year MACE rate was 36.8% in those with CAE and 25.6% in those without CAE.[5] Doi et al. used a narrower composite of cardiac death and nonfatal myocardial infarction and reported MACE in 28.0% of patients with CAE over a median of 49 months.[6]

These cohorts show that CAAE is not a uniform, low-risk angiographic finding. Adverse outcomes have been associated with age, diabetes, renal dysfunction, impaired left ventricular ejection fraction, acute presentation, and greater atherosclerotic burden.[4] A useful assessment after PCI should therefore draw on the clinical information available at discharge, rather than depend on the extent of dilatation or one anatomical classification.

Cai et al. developed a Cox nomogram for 5-year cardiovascular death or nonfatal myocardial infarction in patients with CAE and included quantitative angiographic classification.[7] That work provided an important basis for long-term risk assessment. Its population, however, was limited to CAE; the outcome did not include all-cause death or stroke, and several central predictors required quantitative angiographic measurements. Most other CAAE studies have focused on outcomes, morphology, or treatment associations rather than individual risk after PCI. Direct comparisons of survival prediction approaches under a common evaluation protocol remain scarce.

We therefore compared six candidate survival modelling algorithms using a fixed predictor set and identical patient-level cross-validation partitions. The primary prediction horizon was 3 years. Internal validation of the finalized model-fitting procedure used bootstrap optimism correction, and model performance was evaluated in a temporally distinct cohort without refitting or recalibration.

Methods

Study design and participants

This single-centre retrospective cohort study consecutively included patients with CAAE who were treated at the First Affiliated Hospital of Dalian Medical University between July 2011 and April 2023. Patients admitted from July 2011 through December 2021 formed the development cohort, whereas those admitted from January 2022 through April 2023 formed the temporal validation cohort. Data were obtained from electronic medical records, coronary angiograms, inpatient records, and follow-up information. Reporting followed the TRIPOD+AI statement.[8]

CAAE was identified on the index coronary angiogram. CAA was defined as focal coronary dilatation with a diameter at least 1.5 times that of the adjacent normal reference segment.[1,2] CAE was defined as diffuse dilatation at least 1.5 times the reference diameter, extending for more than 20 mm or involving more than one-third of the vessel length.[1] One physician interpreted all angiograms according to these prespecified criteria and recorded lesion distribution using the Markis classification.

Only the first admission in which CAAE was identified by coronary angiography and PCI was performed was included for each patient. Patients were eligible if they were at least 18 years old, underwent PCI for unstable angina or myocardial infarction, had adequate angiographic information, survived to discharge, and had either an ascertainable outcome or a valid date of last follow-up. Exclusion criteria were severe aortic or other major vascular disease; Kawasaki disease, Takayasu arteritis, or a congenital coronary anomaly; myocardial bridging or another non-atherosclerotic coronary condition; connective tissue disease; an iatrogenic pseudoaneurysm after PCI; or insufficient information to determine angiographic eligibility, outcome status, or follow-up time.

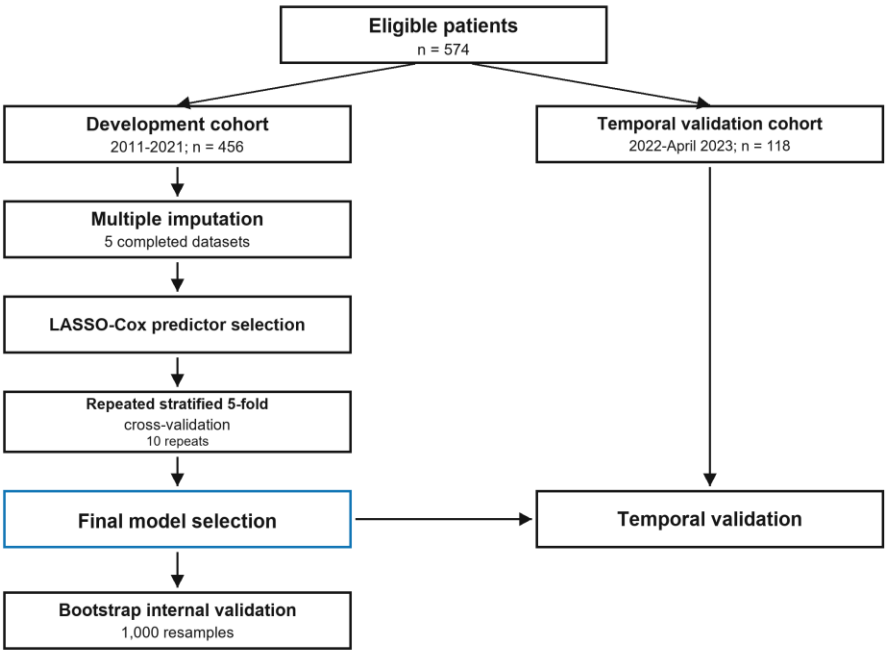


Figure 1. Cohort allocation, model development, and validation workflow.

Candidate predictors

Candidate predictors were obtained during the index admission. They included age; sex; admission diagnosis; hypertension; diabetes; multivessel disease; thrombus aspiration; Markis classification; and discharge treatment with aspirin, ticagrelor, clopidogrel, non–vitamin K antagonist oral anticoagulants (NOACs), statins, ezetimibe, a proprotein convertase subtilisin/kexin type 9 inhibitor, a beta-blocker, nicorandil, or a nitrate. Laboratory and cardiac-function measures were white blood cell count, neutrophil count, lymphocyte count, monocyte count, red blood cell (RBC) count, haemoglobin, platelet count, creatinine, prothrombin time, activated partial thromboplastin time, thrombin time (TT), fibrinogen, D-dimer, B-type natriuretic peptide (BNP), high-sensitivity cardiac troponin I, total cholesterol, triglycerides, high-density lipoprotein cholesterol, low-density lipoprotein cholesterol, glucose, and left ventricular ejection fraction (LVEF). The first measurement obtained after admission was used for laboratory variables and LVEF. The Markis classification describes the extent and distribution of coronary dilatation: type I, diffuse ectasia of two or more vessels; type II, diffuse ectasia in one vessel with localized involvement in another; type III, diffuse ectasia confined to one vessel; and type IV, localized or segmental dilatation of one vessel.[9]

Outcome and follow-up

The primary outcome was the first MACE after hospital discharge, defined as all-cause death, nonfatal myocardial infarction, or nonfatal stroke. MACE occurrence and the date of the first event after discharge were ascertained through a combined review of health insurance records, inpatient medical records, and telephone follow-up. Vital status and dates of death were obtained from health insurance records. Nonfatal myocardial infarction or stroke

reported during telephone follow-up was verified against the corresponding hospitalisation records. All available event information was reviewed to identify the earliest qualifying MACE. Each included patient had either an ascertainable outcome or a valid last follow-up date. Patients with MACE were followed to the first event. Those without an observed MACE were censored on the last date they were confirmed alive and event-free or on 1 May 2026, whichever came first. Potential follow-up was summarized with the reverse Kaplan-Meier method.[10]

Missing data and predictor selection

Missing candidate predictors were handled by multiple imputation by chained equations (MICE).[11] Imputation relationships were estimated in the development cohort only. Five completed datasets were generated using predictive mean matching for continuous variables, with 20 iterations and five donors. The fitted development-cohort imputation relationships were then applied to the temporal validation cohort without re-estimation. Admission date, MACE status, follow-up time, and MACE event type were not included in the imputation predictor matrix. Missingness and convergence diagnostics are provided in Additional file 1, Supplementary Figure S1.

Predictor selection was performed separately in each of the five imputed development datasets using least absolute shrinkage and selection operator (LASSO)-penalized Cox proportional hazards regression (LASSO-Cox).[12] In each dataset, the penalty parameter was selected by stratified 10-fold cross-validation using the minimum cross-validated partial-likelihood deviance criterion (λ_min). Predictors with non-zero coefficients at λ_min in all five imputed datasets were retained according to the prespecified stability rule and carried forward for model development. The predictor set was then fixed and was not altered after candidate-model comparison, bootstrap internal validation, or temporal validation. Detailed selection results are shown in Additional file 1, Supplementary Figure S2.

Model development and selection

Six candidate survival modelling algorithms were compared using the same predictor set: Cox proportional hazards regression, random survival forest (RSF), extra survival trees, gradient boosting survival analysis, a survival support vector machine, and XGBoost with a Cox partial-likelihood objective (XGBoost-Cox).[13-16] Model settings were prespecified before comparison and are reported in Additional file 1, Supplementary Table S2. All data-dependent standardization parameters were estimated within each training fold and applied to the corresponding held-out fold. The development cohort underwent 10 repeats of stratified five-fold cross-validation. Identical patient-level folds were used across all six algorithms and the five imputed datasets. For each held-out fold, patient-level risk scores were averaged across the five imputation-specific models before the C-index was calculated. The algorithm with the highest mean out-of-fold C-index across the 50 folds was selected. Imputation and predictor selection were completed in the

development cohort before repeated cross-validation. The cross-validation results therefore describe algorithm performance conditional on the completed datasets and selected predictors.

Model performance and validation

The final selected model and the reference Cox proportional hazards model were fitted separately in each of the five imputed datasets. Patient-level risk scores and predicted risks were averaged across the five imputation-specific models before cohort-level evaluation. Harrell's C-index quantified discrimination over the entire observed follow-up.[17] Cumulative/dynamic time-dependent AUCs assessed discrimination at 1, 2, and 3 years after discharge, whereas Brier scores quantified overall prediction error at the same time points.[18,19] To account for right censoring, all fixed-time metrics were estimated using inverse probability of censoring weighting (IPCW), with the censoring distribution estimated by the Kaplan-Meier method.

Internal validation of the finalized model-fitting procedure used 1,000 event-stratified, patient-level bootstrap resamples drawn with replacement from the development cohort. Each bootstrap sample contained the same number of observations as the original development cohort. Within each bootstrap replicate, MICE was repeated to generate five imputed datasets, and the fixed RSF and reference Cox models were refitted using identical sampled patient indices. Predictor selection, candidate-algorithm comparison, and hyperparameter tuning were not repeated. Optimism was calculated as performance in the bootstrap sample minus performance when the bootstrap-fitted model was applied to the original development cohort. The optimism-corrected estimate was obtained by subtracting mean optimism from the apparent performance.[20] The optimism correction therefore applied to model fitting with the selected predictors and fixed algorithm settings. It did not account for optimism arising from predictor or algorithm selection.

For temporal validation, the five development-fitted RSF and reference Cox models were applied directly to the temporal cohort. Predictors, model settings, imputation relationships, and risk thresholds remained fixed; no model refitting, hyperparameter tuning, threshold re-estimation, or recalibration was performed. Uncertainty in temporal-validation performance was quantified using 1,000 paired patient-level bootstrap resamples of the temporal cohort, while the development-fitted models remained unchanged. Two-sided percentile 95% CIs were defined by the 2.5th and 97.5th percentiles. Differences between RSF and Cox were calculated within each paired replicate as RSF minus Cox, and two-sided P values were obtained from the proportion of paired bootstrap differences on either side of zero.

Calibration, clinical utility, model interpretation, and risk stratification

At the 3-year horizon, the calibration intercept and slope were estimated using binary logistic recalibration with inverse-probability-of-censoring weights (IPCW), with ideal values of 0 and 1, respectively.[21,22] Development-cohort estimates and grouped calibration points were corrected for optimism using 1,000 bootstrap replicates. The

development-fitted RSF was evaluated in temporal validation without recalibration; patient-level bootstrap resampling of the temporal cohort was used only to derive 95% CIs. Three equally sized groups were used to display calibration points in each cohort. Decision curve analysis was extended to the censored 3-year time-to-event outcome and compared the RSF model with the Cox model and the treat-all and treat-none strategies across threshold probabilities from 0.05 to 0.30.[23,24] Within this analysis, net benefit was estimated using IPCW to account for censoring. Development-cohort curves were corrected for optimism, whereas temporal-validation intervals were derived by patient-level bootstrap resampling without model refitting.

TreeSHAP was used to calculate Shapley additive explanations (SHAP) values for the RSF estimate of 3-year risk. Mean absolute SHAP values summarized global predictor importance.[25] SHAP values were interpreted as contributions to model predictions rather than causal or treatment effects. For risk stratification, tertiles of mean 3-year predicted risk in the development cohort defined low-, intermediate-, and high-risk groups. Kaplan-Meier curves estimated MACE-free survival, and the log-rank test compared the three groups.[26,27] The development-cohort cut points were applied unchanged to temporal validation. Analyses were conducted with Python 3.12.13. Tests were two-sided, and $P < 0.05$ was considered statistically significant.

Use of language model assistance

OpenAI Codex was used in October 2026 to assist with manuscript formatting and alignment with the journal's submission instructions.

Results

Study cohorts and baseline characteristics

The study included 574 patients, of whom 456 entered the development cohort and 118 entered the temporal validation cohort. During the entire follow-up period, 85 patients in the development cohort and 12 in the temporal validation cohort experienced MACE. Of these, 45 and 11 patients, respectively, experienced MACE within 3 years (36 months) after discharge. Median potential follow-up estimated by the reverse Kaplan-Meier method was 97 months (95% CI 92-100) and 41 months (95% CI 39-43), respectively. Both cohorts were predominantly male and most patients had Markis type IV disease. Unstable angina was the most frequent admission diagnosis. The temporal validation cohort differed from the development cohort in diabetes prevalence, several laboratory measures, and use of selected discharge medications (Table 1). Baseline characteristics by MACE status within the development cohort are reported in Additional file 1, Supplementary Table S1.

Table 1. Baseline characteristics of the development and temporal validation cohorts.

Variable	Development cohort, n = 456	Temporal validation cohort, n = 118	Absolute SMD	P value
Age, years	64.00 (56.00-71.25)	66.00 (59.00-71.75)	0.183	0.122
WBC, 10^9/L	7.33 (6.10-9.32)	7.39 (5.80-8.87)	0.030	0.837
Neu, 10^9/L	4.70 (3.72-6.46)	5.03 (3.67-6.26)	0.082	0.699
Lymph, 10^9/L	1.69 (1.29-2.25)	1.73 (1.38-2.12)	0.101	0.904
Mono, 10^9/L	0.52 (0.41-0.68)	0.48 (0.35-0.62)	0.279	0.007
RBC, 10^12/L	4.59 (4.22-4.95)	4.65 (4.27-5.07)	0.137	0.133
Hb, g/L	141.00 (129.00-151.00)	144.50 (133.00-153.00)	0.134	0.167
PLT, 10^9/L	201.50 (171.00-238.75)	210.50 (175.00-246.75)	0.083	0.182
Crea, umol/L	74.00 (63.00-86.00)	74.50 (65.00-89.75)	0.007	0.422
PT, s	11.30 (10.80-11.97)	10.90 (10.40-11.57)	0.045	<0.001
APTT, s	25.10 (22.80-28.40)	24.90 (22.20-27.55)	0.111	0.239
TT, s	16.70 (16.00-17.50)	16.00 (15.40-16.60)	0.129	<0.001
Fib, g/L	2.92 (2.48-3.60)	3.08 (2.56-3.56)	0.078	0.617
D-dimer, mg/L FEU	0.30 (0.18-0.59)	0.29 (0.19-0.53)	0.026	0.935
BNP, ng/L	90.28 (35.55-218.77)	109.49 (40.48-240.42)	0.091	0.408
Hs-cTnI, ug/L	0.31 (0.01-14.21)	0.10 (0.01-4.49)	0.171	0.014
TC, mmol/L	4.73 (4.03-5.48)	4.31 (3.64-5.22)	0.156	0.013
TG, mmol/L	1.52 (1.11-2.14)	1.53 (1.15-2.25)	0.139	0.534
HDL-C, mmol/L	1.03 (0.87-1.22)	1.05 (0.87-1.22)	0.024	0.932
LDL-C, mmol/L	2.73 (2.23-3.26)	2.37 (1.98-3.08)	0.187	0.009
Glu, mmol/L	5.54 (4.90-7.11)	5.90 (5.00-8.20)	0.250	0.035
LVEF, %	57.00 (52.00-59.00)	57.00 (46.00-59.00)	0.208	0.519
Male sex	366 (80.3%)	89 (75.4%)	0.117	0.253
Hypertension	303 (66.4%)	86 (72.9%)	0.140	0.224
Diabetes	110 (24.1%)	45 (38.1%)	0.306	0.003
Multivessel disease	375 (82.2%)	106 (89.8%)	0.220	0.050
Thrombus aspiration	31 (6.8%)	9 (7.6%)	0.032	0.690
Aspirin	423 (92.8%)	93 (78.8%)	0.408	<0.001
Ticagrelor	207 (45.4%)	72 (61.0%)	0.317	0.003

Variable	Development cohort, n = 456	Temporal validation cohort, n = 118	Absolute SMD	P value
Clopidogrel	243 (53.3%)	45 (38.1%)	0.308	0.004
NOACs	14 (3.1%)	11 (9.3%)	0.262	0.009
Statins	445 (97.6%)	117 (99.2%)	0.124	0.475
Ezetimibe	36 (7.9%)	17 (14.4%)	0.208	0.048
PCSK9 inhibitor	9 (2.0%)	20 (16.9%)	0.529	<0.001
Beta-blockers	308 (67.5%)	86 (72.9%)	0.117	0.316
Nicorandil	14 (3.1%)	18 (15.3%)	0.432	<0.001
Nitrate	221 (48.5%)	52 (44.1%)	0.088	0.410
Diagnosis			0.211	0.128
UA	**241 (52.9%)**	**63 (53.4%)**		
NSTEMI	96 (21.1%)	33 (28.0%)		
STEMI	119 (26.1%)	22 (18.6%)		
Markis type			0.163	0.617
I	**4 (0.9%)**	**0 (0.0%)**		
II	8 (1.8%)	2 (1.7%)		
III	24 (5.3%)	4 (3.4%)		
IV	420 (92.1%)	112 (94.9%)		

Note: Continuous variables are presented as median (interquartile range), and categorical variables as n (%). SMD, standardized mean difference.

Predictor selection and model comparison

NOAC use, age, RBC count, creatinine, TT, D-dimer, and BNP were retained by LASSO-Cox regression in all five imputed development datasets (Additional file 1, Supplementary Figure S2). In repeated stratified five-fold cross-validation, RSF had the highest mean out-of-fold C-index, 0.761 (SD 0.038), and was selected according to the prespecified rule (Table 2). XGBoost-Cox ranked second, with a closely similar mean C-index of 0.759 (SD 0.052). This ranking does not establish a meaningful performance difference between the two algorithms.

Table 2. Repeated stratified five-fold cross-validation of six candidate survival modelling algorithms.

Model	Mean C-index	SD	Rank

Model	Mean C-index	SD	Rank
Random survival forest	0.761	0.038	1
XGBoost-Cox	0.759	0.052	2
Extra survival trees	0.756	0.040	3
Gradient boosting survival analysis	0.740	0.048	4
Survival support vector machine	0.731	0.055	5
Cox model	0.724	0.058	6

Note: SD, standard deviation. The SD reflects the 50 repeated out-of-fold C-index results. Ordinary 95% CIs and P values were not calculated because the folds are correlated.

Discrimination and prediction error

After bootstrap correction for optimism, the development-cohort C-index was 0.813 (95% CI 0.782-0.838) for RSF and 0.733 (95% CI 0.675-0.790) for Cox. The paired difference was 0.080 (95% CI 0.028-0.125; P = 0.004). The 3-year AUC was 0.847 (95% CI 0.806-0.881) for RSF and 0.749 (95% CI 0.673-0.826) for Cox, giving a difference of 0.098 (95% CI 0.022-0.163; P = 0.018). The corresponding 3-year Brier scores were 0.077 (95% CI 0.067-0.087) and 0.083 (95% CI 0.069-0.099).

In temporal validation, the C-index was 0.826 (95% CI 0.734-0.910) for RSF and 0.725 (95% CI 0.586-0.845) for Cox. The difference was 0.101 (95% CI -0.004-0.222; P = 0.060). The 3-year AUCs were 0.843 (95% CI 0.742-0.931) and 0.724 (95% CI 0.577-0.857), respectively, with a difference of 0.118 (95% CI 0.009-0.249; P = 0.032). The 3-year Brier scores were 0.071 (95% CI 0.059-0.082) for RSF and 0.082 (95% CI 0.062-0.103) for Cox. Results at 1 and 2 years are presented in Table 3.

Table 3. Performance of RSF and Cox in the development and temporal validation cohorts.

Model	C-index (95% CI)	AUC			Brier score		
		1-year	2-year	3-year	1-year	2-year	3-year
Development cohort							
Cox model	0.733 (0.675-0.790)	0.780 (0.665-0.910)	0.721 (0.621-0.821)	0.749 (0.673-0.826)	0.035 (0.022-0.047)	0.056 (0.039-0.070)	0.083 (0.069-0.099)
RSF model	0.813 (0.782-0.838)	0.875 (0.809-0.927)	0.841 (0.779-0.889)	0.847 (0.806-0.881)	0.035 (0.026-0.046)	0.054 (0.043-0.065)	0.077 (0.067-0.087)
Delta, RSF - Cox (95% CI)	0.080 (0.028-0.125)	0.094 (-0.034-	0.120 (0.019-	0.098 (0.022-	0.000 (-0.005-	-0.002 (-0.008-	-0.006 (-0.015-

Model	C-index (95% CI)	AUC			Brier score		
		1-year	2-year	3-year	1-year	2-year	3-year
		0.193)	0.204)	0.163)	0.007)	0.006)	0.003)
P value	0.004	0.110	0.022	0.018	0.984	0.650	0.184
Temporal validation cohort							
Cox model	0.725 (0.586-0.845)	0.739 (0.469-0.970)	0.712 (0.503-0.881)	0.724 (0.577-0.857)	0.035 (0.020-0.047)	0.053 (0.036-0.069)	0.082 (0.062-0.103)
RSF model	0.826 (0.734-0.910)	0.841 (0.650-0.984)	0.838 (0.723-0.938)	0.843 (0.742-0.931)	0.035 (0.030-0.041)	0.050 (0.044-0.056)	0.071 (0.059-0.082)
Delta, RSF - Cox (95% CI)	0.101 (-0.004-0.222)	0.102 (-0.082-0.340)	0.126 (0.017-0.267)	0.118 (0.009-0.249)	0.001 (-0.010-0.011)	-0.003 (-0.017-0.009)	-0.011 (-0.031-0.004)
P value	0.060	0.476	0.022	0.032	0.934	0.678	0.178

Note: AUCs and Brier scores at 1, 2, and 3 years were estimated using inverse probability of censoring weighting. RSF, random survival forest; AUC, area under the time-dependent receiver operating characteristic curve; C-index, concordance index; CI, confidence interval.

Calibration, clinical utility, model interpretation, and risk stratification

In the development cohort, the optimism-corrected calibration intercept was 0.547 (95% CI -0.557-1.314) and the calibration slope was 1.177 (95% CI 0.213-1.789). In temporal validation, the development-fitted RSF applied without recalibration had an intercept of 0.287 (95% CI -0.539-1.871) and a slope of 1.175 (95% CI 0.700-2.353). In both cohorts, observed risk generally increased with predicted risk across the three grouped calibration points, although intervals were wider in temporal validation (Figure 2).

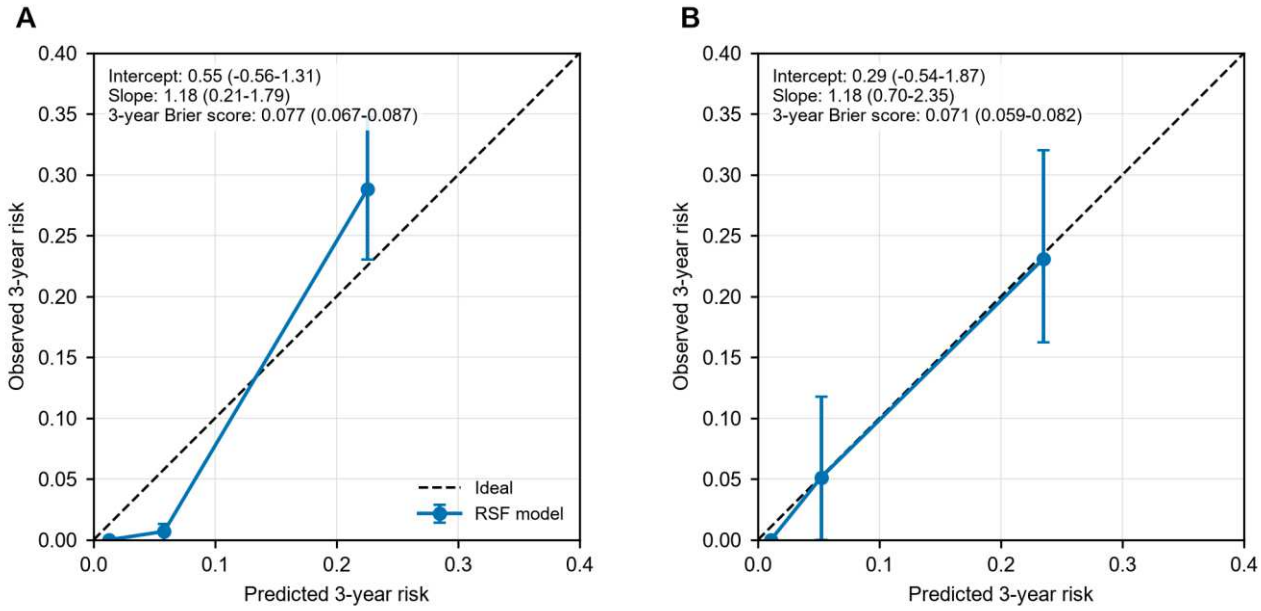


Figure 2. Calibration of the RSF model at 3 years in the development and temporal validation cohorts. Panel A presents bootstrap optimism-corrected development estimates. Panel B presents the development-fitted model applied to temporal validation without recalibration. Points represent three equally sized risk groups; vertical bars indicate 95% CIs. RSF, random survival forest; CI, confidence interval.

Across threshold probabilities from 0.05 to 0.30, RSF produced positive net benefit in both cohorts and exceeded the Cox curve over most of the examined range (Figure 3). SHAP analysis ranked age as the largest average contributor to RSF predictions, followed by D-dimer, TT, BNP, creatinine, and RBC count; NOAC use had the smallest mean absolute SHAP value (Figure 4).

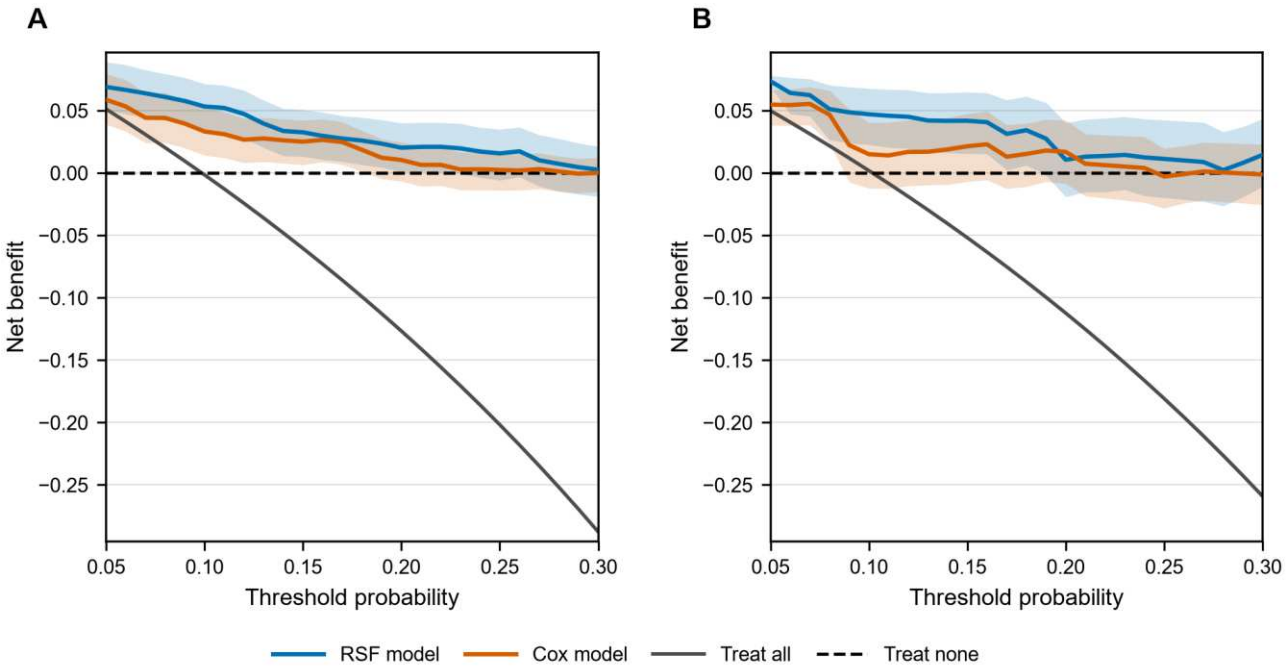


Figure 3. Decision curves at 3 years in the development and temporal validation cohorts. Curves compare RSF, Cox, treat-all, and treat-none strategies over threshold probabilities from 0.05 to 0.30. Model confidence bands represent 95% CIs. RSF, random survival forest; CI, confidence interval.

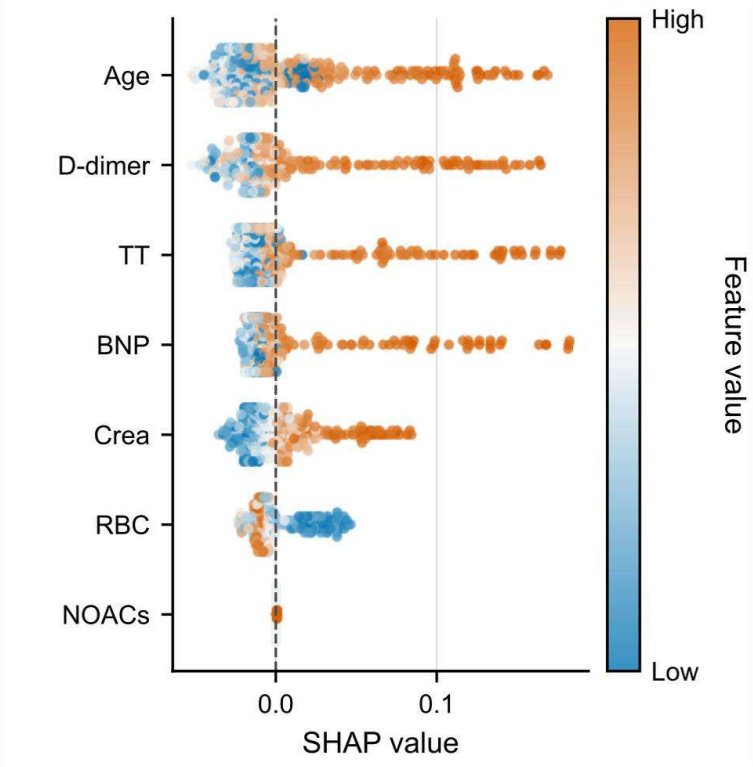


Figure 4. Shapley additive explanations (SHAP) beeswarm plot for the RSF prediction of 3-year MACE risk. Predictors are ordered by mean absolute SHAP value. Colour denotes the relative feature value from low to high. RSF, random survival forest; MACE, major adverse cardiovascular events.

Development-cohort tertiles of 3-year predicted risk defined low-, intermediate-, and high-risk groups. Their 3-year MACE-free survival estimates were 100.0%, 99.3%, and 71.1%, respectively. When the same cut points were applied to temporal validation, the corresponding estimates were 100.0%, 92.1%, and 78.0%. Separation was driven mainly by the high-risk group, whereas low- and intermediate-risk curves were closer. The log-rank P value was <0.001 in the development cohort and 0.0014 in temporal validation (Figure 5 and Additional file 1, Supplementary Table S3). Sensitivity analyses were consistent with the main model; removing NOAC use left the corrected C-index essentially unchanged (Additional file 1, Supplementary Table S4).

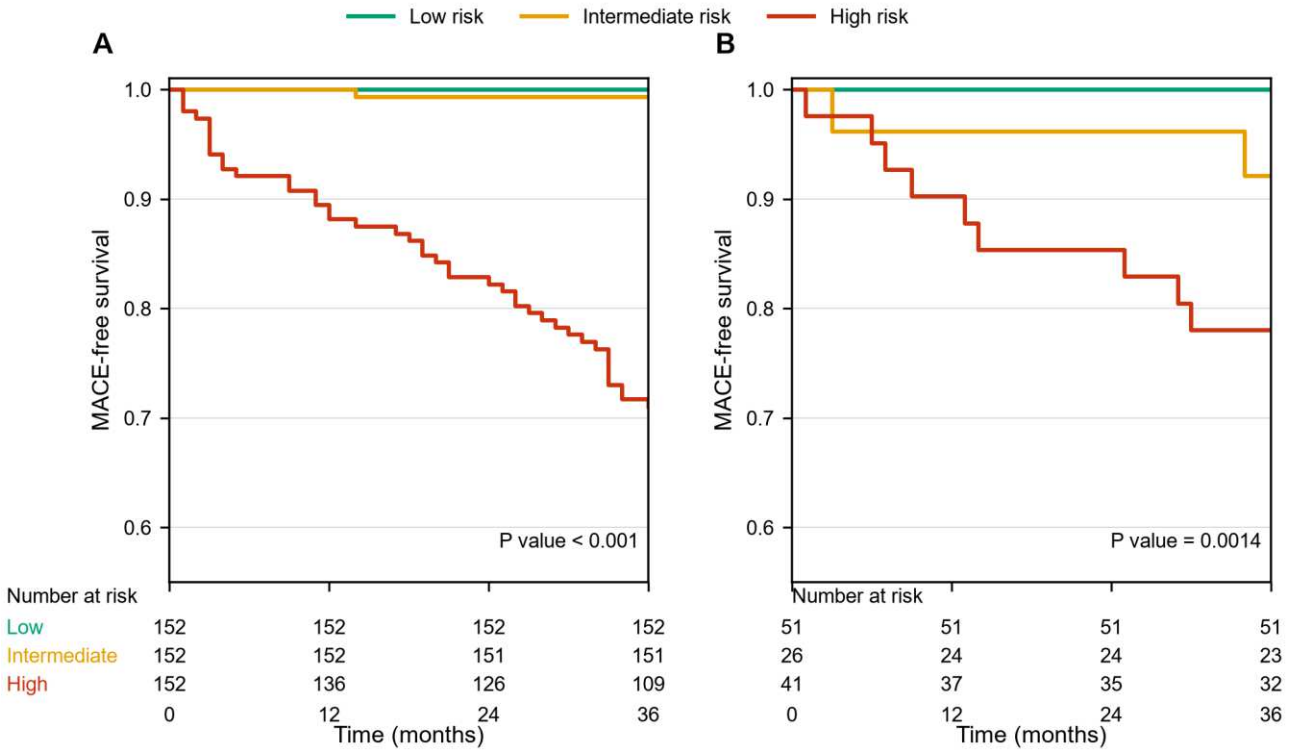


Figure 5. Kaplan-Meier estimates of MACE-free survival by fixed 3-year RSF risk group. Development-cohort tertile thresholds were applied unchanged to temporal validation. Shaded confidence bands were omitted for visual clarity; numbers at risk are shown below each panel. MACE, major adverse cardiovascular events; RSF, random survival forest.

Discussion

We compared six candidate survival modelling algorithms for post-discharge MACE in patients with CAAE who underwent PCI and survived to discharge. RSF was selected according to the prespecified rule because it had the highest mean out-of-fold C-index under the common comparison protocol. Its optimism-corrected C-index and 3-year AUC in the development cohort were 0.813 and 0.847. When applied to the temporal validation cohort without refitting or recalibration, the corresponding estimates were 0.826 and 0.843. RSF had a higher 3-year AUC than Cox in both cohorts, although the C-index difference in temporal validation did not reach statistical significance (P = 0.060).

These findings indicate good discrimination and provide preliminary evidence of performance in later patients from the same centre. Calibration and clinical net benefit require further assessment in larger validation cohorts.

Previous cohorts give a clear clinical reason to estimate risk in CAAE. MACE occurred in 37.1% of patients with CAA in the CAAR registry, in 36.8% of patients with acute myocardial infarction and CAE over 4 years, and in 28.0% of patients with CAE when a narrower cardiac outcome was used.[4-6] CAAE is therefore more than an incidental angiographic description for many patients. Anatomical extent alone, however, cannot represent the wide variation in comorbidity, laboratory findings, presentation, and treatment. A multivariable estimate at discharge may help identify patients who warrant closer surveillance while avoiding the assumption that every patient with an ectatic or aneurysmal segment has the same prognosis.

Earlier studies have examined outcomes in CAE with ST-segment elevation myocardial infarction,[28] diffuse ectatic disease,[29] acute myocardial infarction,[30] and different antithrombotic strategies,[31,32] as well as in CAE accompanied by atherosclerotic coronary disease.[33-35] These studies clarified prognosis and associated risk factors but differed in patient selection, follow-up, and MACE definitions. Most were not designed to estimate long-term risk for an individual patient after PCI. The nomogram reported by Cai et al. addressed prediction more directly, but it was developed for CAE, used cardiovascular death and nonfatal myocardial infarction as the outcome, and incorporated quantitative angiographic features.[7] The present study included both CAA and CAE phenotypes, used a clinically broad MACE outcome, and compared six methods under the same validation design rather than choosing an algorithm in advance.

RSF is an ensemble tree-based method for right-censored time-to-event data that can accommodate nonlinear predictor effects and higher-order interactions without prespecifying their functional forms. This flexibility may be useful when age, renal function, coagulation measures, cardiac stress, and treatment choices are considered together. It offers one plausible explanation for the higher 3-year AUC relative to Cox, although the present analysis cannot determine why the models differed. Temporal validation provided a distinct assessment of performance in later patients. Despite differences in diabetes, laboratory measures, and several discharge medications, the development-fitted RSF retained similar discrimination and prediction error without refitting or recalibration. These findings provide preliminary evidence of temporal transportability within the same centre; performance across institutions remains untested.

The final predictor set consisted of NOAC use, age, RBC count, creatinine, TT, D-dimer, and BNP. All are available from routine inpatient assessment or discharge prescriptions. The relative SHAP contributions were clinically coherent with several features of CAAE. Slow flow and stasis within dilated coronary segments may increase thrombotic and embolic risk, providing context for D-dimer and TT.[1,2] BNP and creatinine may reflect cardiac stress, renal function,

and overall illness burden, while age and RBC count capture additional aspects of physiological reserve. These explanations remain interpretive because SHAP quantifies contribution to a prediction, not biological causation.

NOAC use was retained in all five predictor-selection analyses but had the smallest mean absolute SHAP value. Removing it left the optimism-corrected C-index essentially unchanged. Together, these findings indicate that NOAC use carried some predictive information in the development data but contributed little additional ranking information after the other variables were considered. They do not imply that NOAC use improves or worsens prognosis. Its use is influenced by thrombotic risk, bleeding risk, lesion characteristics, and clinician preference, creating substantial potential for confounding by indication. Because available evidence on antithrombotic treatment in CAE is predominantly observational and remains limited, reported associations should not be interpreted as causal treatment effects.[31,32]

The model separated a group with substantially lower MACE-free survival in both cohorts. The low- and intermediate-risk curves were close, so the three-group scheme is currently more useful for recognizing high-risk patients than for making fine distinctions between the other two groups. Across threshold probabilities from 0.05 to 0.30, decision analysis also suggested net benefit relative to treating all or treating none. In practice, a high estimate could prompt a review of modifiable risks, closer secondary-prevention management, and more frequent follow-up. It should complement clinical assessment, not determine intensified antithrombotic treatment or an interventional strategy on its own.

The study used a chronological cohort split and a consistent protocol for candidate-model comparison. Cohorts were separated by admission date, so temporal validation more closely approximated evaluation in subsequent patients than a random partition. Imputation, predictor selection, and candidate-algorithm comparison were confined to the development period. Each candidate algorithm used the same predictor set and patient-level cross-validation folds, and a prespecified rule determined the final model. Model performance evaluation covered discrimination, calibration, overall prediction error, clinical utility, and risk stratification. The selected predictors are also available in routine inpatient care.

This study has several limitations. Its retrospective, single-centre design limits generalisability, and temporal validation did not assess performance in other institutions or regions. The temporal cohort included only 12 MACE events, of which 11 occurred within 3 years, limiting the precision of performance estimates, particularly calibration and clinical net benefit. Imputation and predictor selection preceded repeated cross-validation. Although imputation and model fitting were repeated during bootstrap validation, predictor selection and candidate-algorithm comparison were not. Internal validation therefore did not capture all sources of optimism in the model-development process. CAAE

classification relied on assessment by one physician, and interobserver agreement was not evaluated. Estimates based on multiple imputation also depend on assumptions about the missing-data mechanism. Unrecorded morphological characteristics, medication doses, adherence, and treatment changes during follow-up may affect predictions and their transportability. Medication-related predictors are susceptible to confounding by indication, and neither their inclusion nor their SHAP contributions should be interpreted as treatment effects. Larger, prospective multicentre studies are needed to assess model performance and clinical usefulness before implementation.

Conclusions

We developed an RSF model using seven routinely available variables to predict post-discharge MACE in patients with CAAE who underwent PCI. The model showed good discrimination and identified a high-risk group, with preliminary evidence from temporal validation at the same centre. Calibration and clinical net benefit require confirmation in larger validation cohorts. Prospective multicentre studies are needed to assess transportability and determine whether model-guided risk assessment improves clinical decisions or patient outcomes.

List of abbreviations

APTT, activated partial thromboplastin time; AUC, area under the curve; BNP, B-type natriuretic peptide; CAA, coronary artery aneurysm; CAAE, coronary artery aneurysm or ectasia; CAE, coronary artery ectasia; CI, confidence interval; C-index, concordance index; Crea, creatinine; DCA, decision curve analysis; Fib, fibrinogen; Glu, glucose; Hb, haemoglobin; HDL-C, high-density lipoprotein cholesterol; hs-cTnI, high-sensitivity cardiac troponin I; IPCW, inverse probability of censoring weighting; LASSO, least absolute shrinkage and selection operator; LDL-C, low-density lipoprotein cholesterol; LVEF, left ventricular ejection fraction; Lymph, lymphocyte count; MACE, major adverse cardiovascular events; MICE, multiple imputation by chained equations; Mono, monocyte count; Neu, neutrophil count; NOAC, non-vitamin K antagonist oral anticoagulant; PCI, percutaneous coronary intervention; PLT, platelet count; PT, prothrombin time; RBC, red blood cell count; RSF, random survival forest; SD, standard deviation; SHAP, Shapley additive explanations; SMD, standardized mean difference; TC, total cholesterol; TG, triglycerides; TT, thrombin time; WBC, white blood cell count.

Declarations

Ethics approval and consent to participate

The study was approved by the Ethics Committee of the First Affiliated Hospital of Dalian Medical University (PJ-KS-KY-2026-468), which waived the requirement for written informed consent.

Consent for publication

Not applicable. The manuscript contains no identifiable individual participant information.

Clinical trial number

Not applicable.

Availability of data and materials

The de-identified datasets generated and/or analysed during the current study are not publicly available because access is subject to ethics and institutional approval, but may be available from the corresponding author on reasonable request and with the required approvals.

Competing interests

The authors declare that they have no competing interests.

Funding

This research was funded by the Noncommunicable Chronic Diseases-National Science and Technology Major Project (project No. 2025ZD0546400; subproject No. 2025ZD0546404); the Natural Science Foundation of Liaoning Province, grant numbers 2024JH2/102500039 and 2025-MSLH-173; the Liaoning Talent Revitalization Program, grant number XLYC2412036; and the Basic Research Project of the Education Department of Liaoning Province, grant numbers LJ232610161004 and LJ222610161004.

Authors' contributions

YL and XD contributed equally to this work. YY and BZ are co-corresponding authors. YL: Conceptualization, Methodology, Investigation, Formal analysis, Data curation, Visualization, Writing - original draft. XD: Conceptualization, Methodology, Investigation, Formal analysis, Validation, Visualization, Writing - original draft. ZD: Investigation, Data curation, Validation. YY: Conceptualization, Supervision, Project administration, Writing - review and editing. BZ: Conceptualization, Supervision, Resources, Funding acquisition, Project administration, Writing - review and editing. All authors read and approved the final manuscript and agreed to its submission.

Acknowledgements

Not applicable.

Additional files

Additional file 1 (DOCX): Supplementary methods, Supplementary Figures S1–S3, and Supplementary Tables S1–S4. See the separately submitted file 'Additional file 1 Supplementary material.docx'.

References

1. Wozniak P, Iwanczyk S, Blaszyk M, Stepien K, Lesiak M, Mularek-Kubzdela T, Araszkiewicz A. Coronary Artery Aneurysm or Ectasia as a Form of Coronary Artery Remodeling: Etiology, Pathogenesis, Diagnostics, Complications, and Treatment. Biomedicines. 2024;12(9):1984. doi:10.3390/biomedicines12091984.
2. Abou Sherif S, Ozden Tok O, Taskoylu O, Goktekin O, Kilic ID. Coronary artery aneurysms: a review of the epidemiology, pathophysiology, diagnosis, and treatment. Front Cardiovasc Med. 2017;4:24. doi:10.3389/fcvm.2017.00024.
3. Luo Y, Tang J, Liu X, Qiu J, Ye Z, Lai Y, et al. Coronary artery aneurysm differs from coronary artery ectasia: angiographic characteristics and cardiovascular risk factor analysis in patients referred for coronary angiography. Angiology. 2017;68(9):823-830. doi:10.1177/0003319716665690.
4. Sánchez-Sánchez I, Cerrato E, Bollati M, Espejo-Paeres C, Nombela-Franco L, Alfonso-Rodríguez E, et al. Long-term prognosis of coronary aneurysms: insights of CAAR, an international registry. JACC Cardiovasc Interv. 2024;17(22):2681-2691. doi:10.1016/j.jcin.2024.08.034.
5. Wang X, Montero-Cabezas JM, Mandurino-Mirizzi A, Hirasawa K, Ajmone Marsan N, Knuuti J, et al. Prevalence and long-term outcomes of patients with coronary artery ectasia presenting with acute myocardial infarction. Am J Cardiol. 2021;156:9-15. doi:10.1016/j.amjcard.2021.06.037.
6. Doi T, Kataoka Y, Noguchi T, Shibata T, Nakashima T, Kawakami S, et al. Coronary artery ectasia predicts future cardiac events in patients with acute myocardial infarction. Arterioscler Thromb Vasc Biol. 2017;37(12):2350-2355. doi:10.1161/ATVBAHA.117.309683.
7. Cai Z, Wang Y, Li L, Wang H, Song C, Yin D, et al. Development and validation of a nomogram for predicting the risk of adverse cardiovascular events in patients with coronary artery ectasia. J Cardiovasc Dev Dis. 2021;8(12):186. doi:10.3390/jcdd8120186.
8. Collins GS, Moons KGM, Dhiman P, Riley RD, Beam AL, Van Calster B, et al. TRIPOD+AI statement: updated guidance for reporting clinical prediction models that use regression or machine learning methods. BMJ. 2024;385:e078378. doi:10.1136/bmj-2023-078378.
9. Markis JE, Joffe CD, Cohn PF, Feen DJ, Herman MV, Gorlin R. Clinical significance of coronary arterial ectasia. Am J Cardiol. 1976;37(2):217-222. doi:10.1016/0002-9149(76)90315-5.
10. Schemper M, Smith TL. A note on quantifying follow-up in studies of failure time. Control Clin Trials. 1996;17(4):343-346. doi:10.1016/0197-2456(96)00075-X.
11. White IR, Royston P, Wood AM. Multiple imputation using chained equations: issues and guidance for practice. Stat Med. 2011;30(4):377-399. doi:10.1002/sim.4067.
12. Tibshirani R. The lasso method for variable selection in the Cox model. Stat Med. 1997;16(4):385-395. doi:10.1002/(SICI)1097-0258(19970228)16:4<385::AID-SIM380>3.0.CO;2-3.
13. Pölsterl S. scikit-survival: a library for time-to-event analysis built on top of scikit-learn. J Mach Learn Res. 2020;21(212):1-6.
14. Ishwaran H, Kogalur UB, Blackstone EH, Lauer MS. Random survival forests. Ann Appl Stat. 2008;2(3):841-860. doi:10.1214/08-AOAS169.

15. Hothorn T, Bühlmann P, Dudoit S, Molinaro A, van der Laan MJ. Survival ensembles. Biostatistics. 2006;7(3):355-373. doi:10.1093/biostatistics/kxj011.

16. Ma B, Yan G, Chai B, Hou X. XGBLC: an improved survival prediction model based on XGBoost. Bioinformatics. 2022;38(2):410-418. doi:10.1093/bioinformatics/btab675.

17. Harrell FE Jr, Lee KL, Mark DB. Multivariable prognostic models: issues in developing models, evaluating assumptions and adequacy, and measuring and reducing errors. Stat Med. 1996;15(4):361-387. doi:10.1002/(SICI)1097-0258(19960229)15:4<361::AID-SIM168>3.0.CO;2-4.

18. Heagerty PJ, Lumley T, Pepe MS. Time-dependent ROC curves for censored survival data and a diagnostic marker. Biometrics. 2000;56(2):337-344. doi:10.1111/j.0006-341X.2000.00337.x.

19. Gerds TA, Schumacher M. Consistent estimation of the expected Brier score in general survival models with right-censored event times. Biom J. 2006;48(6):1029-1040. doi:10.1002/bimj.200610301.

20. Steyerberg EW, Harrell FE Jr, Borsboom GJ, Eijkemans MJC, Vergouwe Y, Habbema JDF. Internal validation of predictive models: efficiency of some procedures for logistic regression analysis. J Clin Epidemiol. 2001;54(8):774-781. doi:10.1016/S0895-4356(01)00341-9.

21. Van Calster B, McLernon DJ, van Smeden M, Wynants L, Steyerberg EW. Calibration: the Achilles heel of predictive analytics. BMC Med. 2019;17:230. doi:10.1186/s12916-019-1466-7.

22. Pate A, Sperrin M, Riley RD, et al. Calibration plots for multistate risk prediction models. Stat Med. 2024;43(14):2830-2852. doi:10.1002/sim.10094.

23. Vickers AJ, Elkin EB. Decision curve analysis: a novel method for evaluating prediction models. Med Decis Making. 2006;26(6):565-574. doi:10.1177/0272989X06295361.

24. Vickers AJ, Cronin AM, Elkin EB, Gonen M. Extensions to decision curve analysis, a novel method for evaluating diagnostic tests, prediction models and molecular markers. BMC Med Inform Decis Mak. 2008;8:53. doi:10.1186/1472-6947-8-53.

25. Lundberg SM, Erion G, Chen H, DeGrave A, Prutkin JM, Nair B, et al. From local explanations to global understanding with explainable AI for trees. Nat Mach Intell. 2020;2(1):56-67. doi:10.1038/s42256-019-0138-9.

26. Kaplan EL, Meier P. Nonparametric estimation from incomplete observations. J Am Stat Assoc. 1958;53(282):457-481. doi:10.1080/01621459.1958.10501452.

27. Mantel N. Evaluation of survival data and two new rank order statistics arising in its consideration. Cancer Chemother Rep. 1966;50(3):163-170. PMID:5910392.

28. Baldi C, Silverio A, Esposito L, Di Maio M, Tarantino F, De Angelis E, et al. Clinical outcome of patients with ST-elevation myocardial infarction and angiographic evidence of coronary artery ectasia. Catheter Cardiovasc Interv. 2022;99(2):340-347. doi:10.1002/ccd.29738.

29. Cai Z, Liu J, Wang H, Yin D, Song W, Dou K. Diffuse coronary artery dilation predicted worse long-term outcomes in patients with coronary artery ectasia. Int J Cardiol. 2020;319:20-25. doi:10.1016/j.ijcard.2020.05.054.

30. Eid MM, Mostafa MR, Alabdouh A, AbdelQadir YH, Mohamed S, Abdelazeem B, et al. Long-term outcomes of acute myocardial infarction in pre-existing coronary artery ectasia: a systematic review and meta-analysis. Curr Probl Cardiol. 2023;48(5):101626. doi:10.1016/j.cpcardiol.2023.101626.

31. Esposito L, Di Maio M, Silverio A, Cancro FP, Bellino M, Attisano T, et al. Treatment and outcome of patients with coronary artery ectasia: current evidence and novel opportunities for an old dilemma. Front Cardiovasc Med. 2022;8:805727. doi:10.3389/fcvm.2021.805727.

32. Gunasekaran P, Stanojevic D, Drees T, Fritzlen J, Haghnegahdar M, McCullough M, et al. Prognostic significance, angiographic characteristics and impact of antithrombotic and anticoagulant therapy on outcomes in high versus low grade coronary artery ectasia: a long-term follow-up study. Catheter Cardiovasc Interv. 2019;93(7):1219-1227. doi:10.1002/ccd.27929.

33. Willner NA, Ehrenberg S, Musallam A, Roguin A. Coronary artery ectasia: prevalence, angiographic characteristics and clinical outcome. Open Heart. 2020;7(1):e001096. doi:10.1136/openhrt-2019-001096.

34. Xi Z, Qiu H, Guo T, Wang Y, Dou K, Xu B, et al. Prevalence, predictors, and impact of coronary artery ectasia in patients with atherosclerotic heart disease. Angiology. 2023;74(1):47-54. doi:10.1177/00033197221091644.

35. Liu H, Gao X, Liang G, Zhao J. Five-years' prognostic analysis for coronary artery ectasia patients with coronary atherosclerosis: a retrospective cohort study. Front Cardiovasc Med. 2022;9:950291. doi:10.3389/fcvm.2022.950291.

Supplementary Files

This is a list of supplementary files associated with this preprint. Click to download.

- Additionalfile1Supplementarymaterial.docx